Journal of Science and Technology – Smart Systems and Devices
Volume xx, Issue x, Month 2026, ppp-ppp

Discriminating Natural and Ethephon-Induced Ripening in Bananas via Electrochemical Impedance Spectroscopy (EIS)

***Hau Tran Thi*[1,*], *Son Nguyen Ky*[1], *Hai Pham Ngoc*[1], *Giang Chu Hoang*[1], *Phu Nguyen Trung*[2]**

[1]*Hanoi University of Science and Technology, Ha Noi, Vietnam*
[2]*Vietnam National University, Ha Noi, Vietnam*
[*]*Corresponding author email: hau.tranthi@hust.edu.vn*

Abstract

This paper presents a non-invasive approach for monitoring the ripening process and detecting artificial ripening methods in bananas (Musa paradisiaca) using Electrochemical Impedance Spectroscopy (EIS). While Ethephon is widely used to accelerate ripening, distinguishing between naturally and chemically ripened fruit remains a challenge. In this study, impedance measurements on Musa paradisiaca were conducted over a 7-day period across a frequency range of 50Hz to 1MHz using surface electrodes to maintain tissue integrity. The results demonstrated that samples treated with 1,000ppm Ethephon exhibited a stable and progressive increase in real impedance (Zreal), peaking at approximately 60,000Ω by Day 6. A distinct "impedance collapse" phenomenon was identified in overdosed samples (2,000 ppm), serving as a clear electrical marker to differentiate forced ripening from natural processes. To quantify those physiological changes, an equivalent circuit model was implemented, showing high concordance with experimental Nyquist plots. The findings confirm that EIS parameters, particularly charge transfer resistance and Warburg diffusion, serve as reliable, non-destructive indicators for further research fruit quality assessment and the detection of forced ripening.

Keywords: Electrochemical impedance spectroscopy (EIS), equivalent circuit modeling, ethephon detection, fruit ripening, non-invasive measurement.

1. Introduction

Electrical Impedance Spectroscopy (EIS) has emerged as a promising technique in the field of food quality assessment, demonstrating significant success in the evaluation of animal-derived proteins. Numerous studies have reported the high sensitivity of EIS in monitoring the freshness of meat and fish, where changes in cellular structure and ionic conductivity serve as reliable indicators of quality. Grossi and Riccò (2017) confirmed that EIS is a cost-effective, rapid, and non-destructive tool for agricultural quality assessment. Their work showed strong correlations between electrical parameters, such as impedance magnitude and phase angle, and internal physiological changes associated with cellular integrity, highlighting the potential of EIS for automated quality sorting systems [1].

Kertész *et al.* (2015) further explored practical applications of impedance spectroscopy for food quality monitoring, showing that multi-frequency complex impedance measurements enable the non-destructive detection of internal structural changes and moisture variations during drying [2]. Recent studies have validated the effectiveness of EIS in evaluating key meat quality parameters. Zhao *et al.* (2017) demonstrated that dielectric properties from impedance measurements strongly correlate with traditional quality indicators such as pH and tenderness, providing a rapid solution for real-time monitoring in meat processing environments [3]. Similarly, Damez *et al.* (2007) employed Bioelectrical Impedance Spectroscopy (BIS) to analyze temporal changes in tissue electrical behavior, confirming its high sensitivity to cellular degradation and ionic redistribution during post-mortem storage [4].

Beyond application-oriented studies, Nguyen Phan Kien introduced a bio-impedance measurement framework by optimizing signal processing and hardware integration to improve dielectric response accuracy while reducing measurement noise [5]. This was subsequently upgraded into a specialized system for meat quality analysis, enhancing measurement stability and enabling the detection of additives and evaluation of water-holding capacity in pork and chicken [6]. These pioneering works established that the complex impedance of biological tissues is not a static physical parameter, but a dynamic indicator of cellular health and chemical purity.

From these advances in meat science, the application of EIS has expanded toward the botanical domain. While the fundamental principle of measuring dielectric properties remains consistent, fruit tissues present distinct challenges due to their complex cell wall structures and starch-to-sugar conversion during ripening. Unlike animal tissues, plant cells possess

p-ISSN 3093-3285
e-ISSN 3093-3315
https://doi.org/10.51316/jst.xxx.ssad.2026.xx.x.x
Received: Mar 1, 2026; Revised: May 6, 2026;
Accepted: Jun 3, 2026; Online: Jul 27, 2026

rigid cellulosic walls and large central vacuoles, which dominate the dielectric response within specific frequency ranges [7]. Although various EIS configurations have been explored for fruit quality assessment, most existing studies rely on invasive needle electrodes, which disrupt fruit tissue integrity and induce stress-related physiological responses, potentially skewing impedance measurements [8].

Bananas (Musa spp.) are among the most important climacteric fruits in global trade, including Vietnam. During ripening, bananas undergo substantial changes, including pulp softening, starch-to-sugar conversion, and chlorophyl degradation [9]. According to the Ministry of Agriculture and Rural Development (MARD), banana production in Vietnam has reached approximately 2.3–2.5 million tons annually, with a total cultivation area exceeding 150,000 hectares [10]. This large production scale highlights the banana's economic significance and its role as a key income source for farmers, while its high nutritional value necessitates rigorous quality and safety control.

The widespread of artificial ripening agents has raised concerns regarding food safety. Ethephon (2-chloroethylphosphonic acid) is the most commonly used ripening agent due to its ability to release ethylene gas within fruit tissues [11]. Chemically, it bypasses the fruit's natural regulatory mechanisms, forcing a rapid surge in respiration. This so-called "chemical shock" can result in uneven nutrient distribution and, in cases of over-dosage, leave acidic residues that compromise the fruit's pH balance. In contrast to the natural ripening, Ethephon-induced ripening accelerates cell wall degradation and alters metabolic profiles [12]. As a result, Ethephon-treated bananas often achieve a visual indistinguishable from naturally ripened fruit, while having inferior flavor complexity and reduced nutritional density. This presents a challenge for both consumers and authorities, highlighting the need for objective and reliable methods to assess fruit quality and ripening provenance.

Conventionally, ripening assessment and chemical residue detection rely on destructive mechanical tests, such as the Magness–Taylor firmness measurement, or advanced analytical techniques including High-Performance Liquid Chromatography (HPLC) and Gas Chromatography (GC) [13]. Although these methods provide high precision, they are destructive, cost-intensive, and unsuitable for real-time, high-throughput monitoring within modern supply chains. Electrical Impedance Spectroscopy offers an alternative by examining the dielectric characteristics of tissues. The interaction between an applied alternating current and cellular structures produces a "biological fingerprint" reflecting the physiological state of the fruit [14]. In plant tissues, impedance responses are strongly frequency-dependent: at low frequencies, current is confined to extracellular pathways, whereas at higher frequencies it penetrates cell membranes acting as biological capacitors [7]. Ripening-related membrane degradation and ionic leakage have been shown to significantly alter impedance spectra [15]. However, most previous EIS studies on fruit employ invasive needle electrodes, which cause physical damage and induce wound responses that can distort data and generate false-positive ripening indicators [8].

To address this limitation, the study employs a non-invasive measurement approach using flexible surface electrodes. This approach enables the acquisition of impedance signatures without inducing tissue stress, thereby improving measurement reliability compared to invasive methods. More importantly, it allows the identification of a distinct "impedance collapse" phenomenon under Ethephon overdose, which serves as a novel electrical marker to differentiate forced ripening from natural processes. In this study, we evaluate the effectiveness of Electrical Impedance Spectroscopy as a diagnostic tool for differentiating naturally ripened bananas from Ethephon-treated bananas at 1,000ppm and 2,000ppm concentrations. Impedance measurements are conducted across a frequency range from 50Hz to 1MHz [12]. The results aim to establish a quantitative, non-destructive proof-of-concept for banana quality assessment and chemical ripening detection in agrifood applications.

2. Materials and Methods

2.1. Sample Preparation and Classification

This study utilized *Musa paradisiaca* (locally known as "Chuối Tây"), a widely consumed banana variety in Vietnam. Experimental samples were selected under strict criteria: a single bunch of 15 dark-green bananas was procured approximately three hours post-harvest. From this bunch, twelve fruits were selected for the experiment. Before testing, all specimens were cleansed with a saline solution to remove surface impurities.

The samples were divided into three experimental groups ($n = 4$):

- **Group 1 (Control - Samples 1, 2, 3, 4):** Fruits allowed to ripen naturally at room temperature (25°C, relative humidity 50–70%).
- **Group 2 (Standard Ethephon - Samples 1.1, 2.1, 3.1, 4.1):** Fruits submerged in a 1,000 ppm Ethephon solution (recommended dose for stable physiological ripening) for 4 minutes.
- **Group 3 (Overdose Ethephon - Samples 1.2, 2.2, 3.2, 4.2):** Fruits treated with a 2,000 ppm Ethephon solution to simulate forced ripening and investigate structural cell damage under excessive chemical influence.

Fig. 1. Three groups of Bananas

2.2. Chemical Mechanisms of Artificial Ripening

This research employed Ethephon (2.5%) as the artificial ripening agent. Upon absorption into the fruit tissue, Ethephon undergoes hydrolysis, releasing ethylene (C_2H_4) gas along with free ions (Cl^- and $H_2PO_4^-$). It acts as a natural plant hormone that regulates ripening through the following reaction:

$$Cl-CH_2-CH_2-PO_3H_2+OH^- \rightarrow C_2H_4\uparrow+Cl^-+H_2PO_4^-$$

High concentrations of ethylene, particularly at 2,000 ppm, significantly accelerate enzymatic activities. Specifically, Amylase facilitates the rapid hydrolysis of starch into sugars, while Pectinase degrades the pectin in the cell walls, leading to tissue softening. These transformations alter the dielectric properties of the fruit, which can be captured via Electrical Impedance Spectroscopy (EIS).

Fig. 2. Ethephon 2.5% solution used for the experiment

2.3. Non-Invasive Impedance Measurement System

2.3.1. Impedance analyzer

The electrical parameters, specifically impedance magnitude ($|Z|$) and phase angle, were acquired using a HIOKI IM3570 Impedance Analyzer (Fig. 3). The instrument allows high-precision analysis of complex parameters including Z, R, L, C, ESR, and dissipation factor ($\tan\delta$) (Fig. 4).

2.3.2. Electrode interface

To establish a stable connection between the banana and the analyzer, disposable Ag/AgCl electrodes were utilized (Fig. 5). These electrodes feature a wet gel layer that effectively reduces contact impedance and enhances signal stability (Fig. 6). The Ag/AgCl material is preferred in bio-impedance studies as it minimizes electrode polarization effects at low frequencies. By avoiding penetration of the fruit's peel, the internal pulp remains unexposed to air, preventing induced stress or premature oxidation that could interfere with the ripening process.

Fig. 3. Impedance analyzer mode selection

Fig. 4. Impedance analyzer configuration

Fig. 5. Experiment setup #1

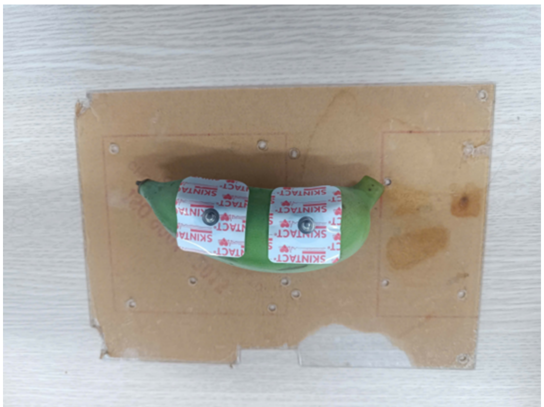

Fig. 6. Experiment setup #2

2.3.3. Measurement protocol

The electrical impedance characteristics of the samples were acquired using HIOKI IM3570 Impedance Analyzer. To capture the full dielectric response, the device was configured in Analyzer Mode with a logarithmic frequency sweep ranging from 50Hz to 1MHz. A low frequency is critical for characterizing electrode polarization and extracellular resistance (R_e), as the high capacitive reactance of the cell membranes effectively blocks current from entering intracellular space. As the frequency increases into the mid-range (1kHz to 100kHz), the phenomenon of Beta dispersion occurs, where the current penetrates the cell membranes, making this range highly sensitive to the enzymatic degradation of pectin & starch induced by Ethephon. Lastly, the high-frequency extension up to 1 MHz allows the measurement of intracellular resistance (R_i) and the total electrolyte conductivity. This wide bandwidth ensures that the transition from a resistive extracellular path to a combined intracellular-extracellular path is fully captured, provides a holistic view of the structural integrity of the fruit during the accelerated ripening process.

A constant current of 0.5mA was selected to maintain a linear relationship between voltage and current throughout the measurement. In biological tissue analysis, it is imperative to operate within the linear region of the specimen's I-V characteristic. A constant voltage level of 0.5mA is sufficiently high to provide an adequate signal-to-noise ratio (SNR), overcoming the inherent contact impedance of the banana peel and the electrode interface. Conversely, it is also low enough to prevent non-linear bio-electrochemical effects, such as the irreversible breakdown of cell membranes (electroporation) or the induction of significant ion migration (electrophoresis).

To minimize stochastic noise and electromagnetic interference, a "SLOW1" measurement speed was utilized with an averaging factor of four. Prior to each session, standardized Open and Short compensation procedures were executed to nullify parasitic capacitance and residual lead inductance, ensuring the measurements reflected only the impedance of the specimen. To eliminate the influence of lead wire resistance and contact impedance at the terminals, a 4-terminal Kelvin connection was implemented. This configuration utilizes separate pairs of leads for current excitation (H_{cur}, L_{cur}) and voltage sensing (H_{pot}, L_{pot}), allowing for the precise acquisition of the complex impedance magnitude ($|Z|$) and phase angle (θ) directly from the target tissue area.

2.3.4. Data acquisition

Impedance spectroscopy data were collected every 24 hours over a 6-day period (Impedance data collection commenced on Day 2, 24 hours after Ethephon treatment). The results were exported in .csv format for further calculation and equivalent circuit modeling. The experimental data were fitted to a modified Hayden model incorporating a Constant Phase Element (CPE) to account for the non-ideal capacitive behavior of the cell membranes and the heterogeneous structure of the peel. All measurements were conducted at a controlled room temperature of 25°C.

The measurement procedure followed a standardized four-step workflow:

- **Step 1 (Sample Selection):** 12 bananas were selected from one single bunch. Those chosen were as identical in shape, weight, length and size as possible.
- **Step 2 (Sample Preparation):** Each banana was cleaned, and two electrodes were attached to the surface. The electrodes were positioned on the same side of the fruit, spaced approximately 4 cm apart (measured from the center of each electrode), and 3–5 cm from the stem end.
- **Step 3 (Data Acquisition):** Measurements were performed using the pre-configured parameters on the HIOKI IM3570.
- **Step 4 (Data Export):** The acquired datasets were saved in .csv format and extracted via USB.

2.3.5. Data processing

After obtaining raw data, we proceeded to process and analyze the dataset. Euler's formula represents the complex exponential:

$$e^{j\omega} = \cos\omega + j\sin\omega \tag{1}$$

Applying the voltage divider principle to the measurement model, the complex impedance Z can be expressed as:

$$Z = R_1\left(\frac{v_1 e^{j\omega}}{v_2 e^{j\omega}} - 1\right)^{-1} \tag{2}$$

This formula can then be converted to:

$$Z = R_1 \cdot \frac{v_2}{v_1} \cdot \frac{1}{\cos\omega + j\sin\omega - \frac{v_2}{v_1}} \tag{3}$$

$$Z = R_1 \cdot \frac{v_2}{v_1} \cdot \frac{\cos\omega - \frac{v_2}{v_1} - j\sin\omega}{\left(\cos\omega - \frac{v_2}{v_1}\right)^2 + \sin^2\omega} \quad (4)$$

Accordingly, the real and imaginary components of the impedance are obtained as follows:

$$Re(Z) = R_1 \cdot \frac{v_2}{v_1} \cdot \frac{\cos\omega - \frac{v_2}{v_1}}{\left(\cos\omega - \frac{v_2}{v_1}\right)^2 + \sin^2\omega} \quad (5)$$

$$Im(Z) = R_1 \cdot \frac{v_2}{v_1} \cdot \frac{-\sin\omega}{\left(\cos\omega - \frac{v_2}{v_1}\right)^2 + \sin^2\omega} \quad (6)$$

After visualizing the frequency response and impedance characteristics, we were able to recreate the corresponding electrical components of the samples based on the features and attributes of each electric element:

- **Resistor (R):** Resistor with resistance R (Ω) contributes to the real part of impedance: $Z(\omega) = R$.
- **Constant Phase Element (CPE):** CPE is an element used often in modeling the AC response of non-homogeneous systems. CPE has two parameters: Q and n, given by the formula:

  $$Z_{CPE}(\omega) = Q^{-1}(j\omega)^{-n} \quad (7)$$

  Q becomes equal to capacitance when $n = 1$. Similarly to a capacitor, CPE keeps the phase constant at variable frequency but the phase shift differs from 90°. CPE is especially helpful for representing slightly distorted capacitances.
- **Warburg (W):** Impedance of finite-length diffusion with reflective boundary. This element has two parameters: W_r and W_c. Impedance of W element is:

  $$Z_W(\omega) = W_r \cdot \omega^{-1/2}(1-j)\coth(W_c\sqrt{j\omega}) \quad (8)$$

The experimental data were modeled using an equivalent electrical circuit to quantify the physiological changes during ripening (Fig. 7). In this configuration, the resistor R_0 represents extracellular fluid resistance, where a decrease indicates ion release due to cell wall degradation. $R_l \parallel L$ accounts for high-frequency responses associated with vascular structures and measurement interface effects. The core of the model is the $R \parallel CPE$ combination, where they characterize the non-ideal capacitive properties of the lipid bilayer; variations in these parameters serve as primary indicators of membrane integrity. Finally, a semi-infinite Warburg impedance (W) is incorporated to describe ion diffusion within the parenchyma, providing insights into starch-to-sugar conversion and rheological transitions.

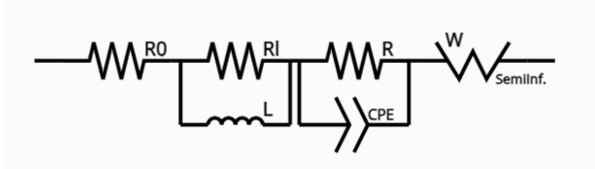

Fig. 7. Equivalent Circuit

3. Results

Figures 8 to 13 illustrate the changes in the specimens during the 7-day period. These observable transitions correlate with the variations captured in the measured impedance magnitude and phase angle.

Fig. 8. Experiment subjects at Day 2

Fig. 9. Experiment subjects at Day 3

Fig. 10. Experiment subjects at Day 4

Fig. 11. Experiment subjects at Day 5

Fig. 12. Experiment subjects at Day 6

Fig. 13. Experiment subjects at Day 7

Through Fig. 14 and Fig. 15, the electrochemical behavior of banana tissue under different Ethephon concentrations over a 7-day ripening cycle is characterized using impedance magnitude ($|Z|$) and phase angle (θ). The impedance magnitude reflects the overall resistive behavior of the tissue, while the phase angle indicates capacitive properties associated with cell membrane integrity. The control group (no Ethephon) exhibited the lowest $|Z|$ values and the least negative phase angles throughout the experiment, indicating a slow and stable natural ripening process with minimal changes in membrane-related dielectric properties. The 1,000ppm Ethephon-treated group showed a well-defined and progressive impedance response. From Day 4 onward, $|Z|$ increased steadily and reached maximum values during Days 5–7, while the phase angle displayed pronounced negative troughs in the mid-frequency range. These results indicate effective stimulation of starch-to-sugar conversion and ionic redistribution while preserving membrane integrity, allowing the cell membranes to function as a stable dielectric barrier.

In contrast, the 2,000ppm group exhibited an intense but transient response. A sharp increase in $|Z|$ and the most negative phase angle were observed on Day 2, followed by a significant decline from Day 4 onward. By Day 7, the impedance characteristics converged toward those of the control group, suggesting over-ripening and early senescence.

This behavior is attributed to membrane degradation and increased permeability, leading to electrolyte leakage and reduced insulation capacity. The most pronounced differentiation among treatments occurred in the low-frequency region ($< 10^3$ Hz), which is highly sensitive to extracellular resistance and membrane condition. Overall, the results confirm that 1,000ppm Ethephon represents an optimal concentration for maintaining a stable and distinguishable electrochemical signature, enabling reliable ripening classification using EIS.

As illustrated in Fig. 16, the real part of the complex impedance (Z_{real}) of all banana samples exhibits a consistent inverse relationship with frequency over the ripening period from Day 2 to Day 7. Under all experimental conditions, Z_{real} reaches its maximum value in the low-frequency region (below 10^3 Hz) and gradually converges toward a common minimum as the frequency approaches 10^6 Hz. This convergence indicates that high-frequency currents bypass membrane capacitance and are dominated by electrolyte resistance.

During the early ripening stage (Day 2–Day 3), impedance profiles for all treatments remain closely grouped. A clear separation appears from Day 4 onward, where the 1,000ppm Ethephon-treated samples exhibit a marked increase in low-frequency Z_{real}, reaching approximately 60,000Ω by Day 6–Day 7. The 2,000ppm treatment shows a lower and more moderate impedance response during the same period. These results suggest that Ethephon concentration significantly influences tissue structure and ion transport behavior. The elevated Z_{real} observed in the 1,000ppm group is likely associated with starch degradation and changes in cellular permeability, which modify ionic mobility within the fruit tissue.

Fig. 17 presents the frequency-dependent behavior of the imaginary impedance (Z_{imag}) for banana samples under different Ethephon treatments from Day 2 to Day 7. All spectra display a characteristic peak-shaped

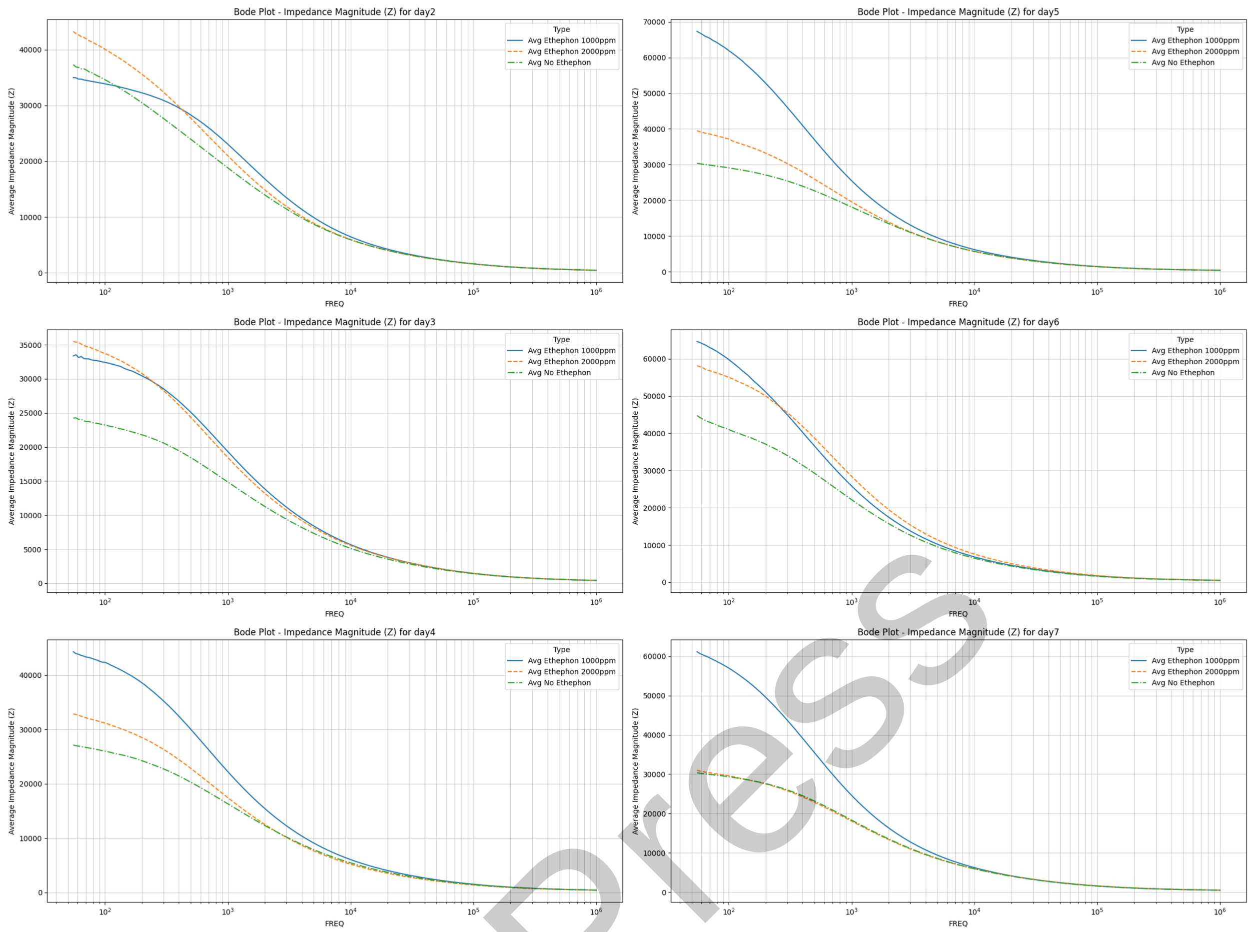

Fig. 14. Magnitude bode plot over 6 days

profile, reflecting the capacitive nature of biological tissues due to cell membranes acting as leaky capacitors. Across all days, Z_{imag} reaches a maximum in the intermediate frequency range (10^2–10^3 Hz), where membrane polarization effects are most prominent. At high frequencies (> 10^5 Hz), Z_{imag} values converge toward zero, indicating that membrane reactance is bypassed and current flow is dominated by electrolyte conductivity.

In the early stage (Day 2–3), the 2,000ppm Ethephon-treated samples exhibit the highest capacitive peak, while the control group shows the weakest response. From Day 4 onward, the 1,000ppm group maintains a strong and stable Z_{imag} peak, whereas the 2,000ppm group shows a noticeable reduction in peak magnitude, suggesting membrane degradation and increased permeability due to over-ripening. These results demonstrate that Z_{imag} is highly sensitive to membrane integrity and Ethephon concentration, with 1,000ppm providing the most distinct and stable capacitive response for EIS-based ripening assessment.

With the equivalent circuit model, the parameters of the circuit components are shown in Table 1:

Table 1. Parameters of the circuit components

Circuit Parameter	Value
R0	300 Ω
R1	200 Ω
L1	1e-6 H
R2	58,000 Ω
CPE1_Q	1.2e-8
CPE1_n	0.9
W1	12,000

- **R0 = 300.0:** Estimated from the Z_{real} intercept at high frequencies, where the Nyquist arc starts near the origin.
- **R1 = 200.0 & L1 = 1e-6:** Included to compensate for high-frequency inductive artifacts or phase shifts common in biological EIS measurements.
- **R2 = 58,000.0:** Represents the transfer resistance charge, matching the large arc diameter of the 1000 ppm sample on Day 7 (approx. 60k Ω).

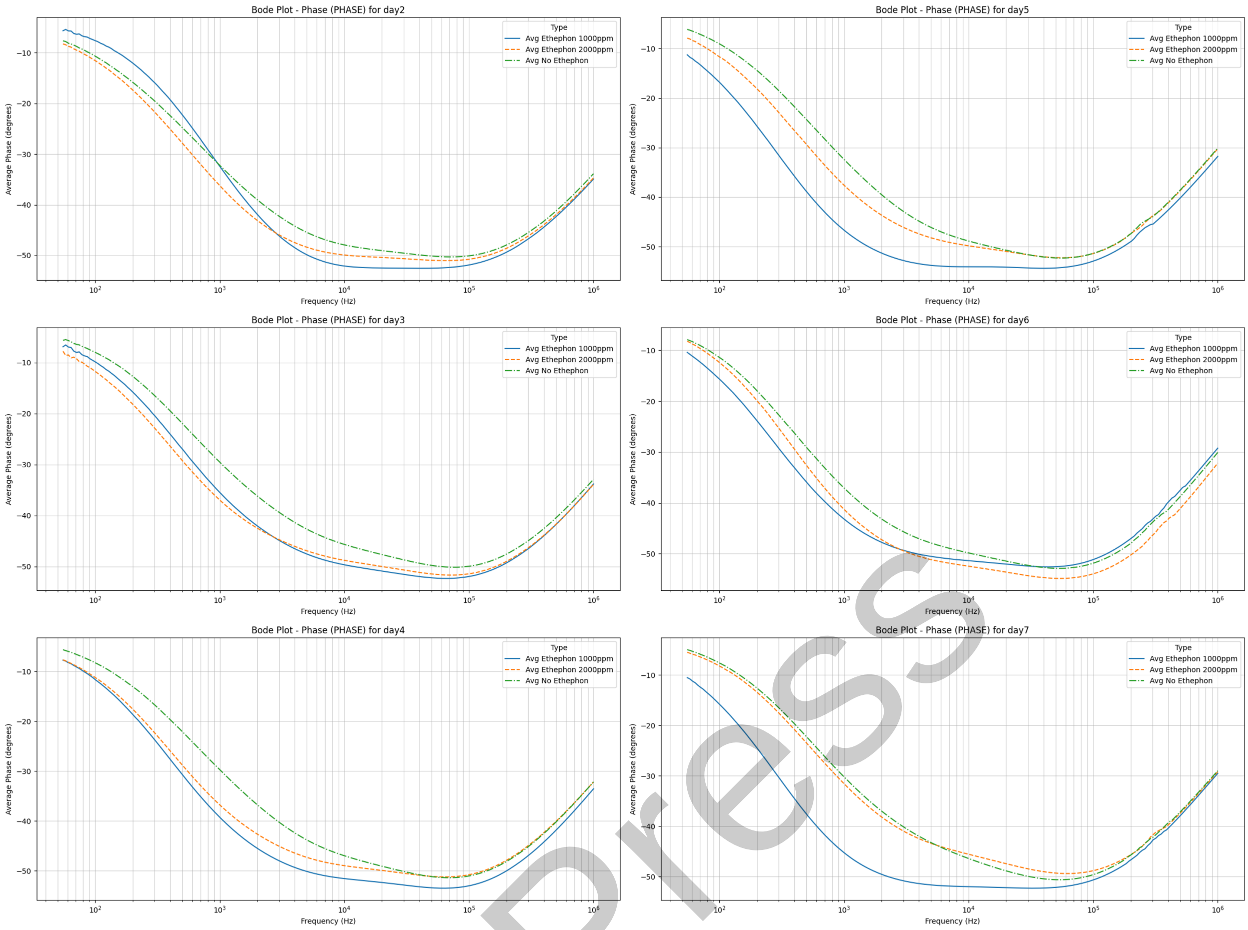

Fig. 15. Phase plot over 6 days

- **CPE1_Q = 1.2e-8 & CPE1_n = 0.9:** Reflects the non-ideal capacitance of cell membranes ($n < 1$), causing the "depressed" arc shape observed in the plots.
- **W1 = 1200.0:** Accounts for the semi-infinite diffusion (Warburg impedance) of ions and metabolites within the fruit tissue at low frequencies.

Fig. 18 validates the equivalent circuit model against experimental Nyquist plots, demonstrating high concordance in tracking the structural evolution of banana samples. While initial profiles (Days 2–3) showed uniformity, a divergence emerged at Day 4 as the 1,000ppm sample exhibited a significant impedance rise, peaking above 60,000Ω due to starch-to-sugar conversion. In contrast, Day 7 marked a rapid impedance drop to approximately 30,000Ω in the 2,000ppm and control groups, indicating early senescence characterized by membrane degradation and increased ion mobility. The 1,000ppm sample, however, maintained stability with a sustained high impedance arc. The model's accuracy, particularly in the Warburg tail and inductive regions, confirms its effectiveness in characterizing the differential ripening kinetics and dielectric behavior under varying Ethephon concentrations.

4. Discussion

The experimental results provide a clear differentiation between the impact mechanisms of varying Ethephon concentrations on the cellular architecture of *Musa paradisiaca* through their distinct electrical impedance signatures. The observed divergence in dielectric behavior offers profound insights into the physiological transitions occurring within the fruit tissue during accelerated ripening.

4.1. Biophysical Implications of Ripening Mechanisms

The maintenance of a stable impedance profile in the control and 1,000ppm groups suggests a controlled metabolic transition. During this phase, the hydrolysis of starch into soluble sugars increases the osmotic pressure within the parenchyma cells, yet the structural integrity of the lipid bilayer remains largely intact. This allows the cell membranes to continue acting as effective biological capacitors, as evidenced by the sustained Nyquist arcs and stable phase angle troughs.

In stark contrast, the "impedance collapse" observed in the 2,000ppm overdosed group, where the real impedance dropped significantly by Day 7, indicates a state of early senescence. Physiologically, this reduction reflects the abrupt disruption of the lipid membrane

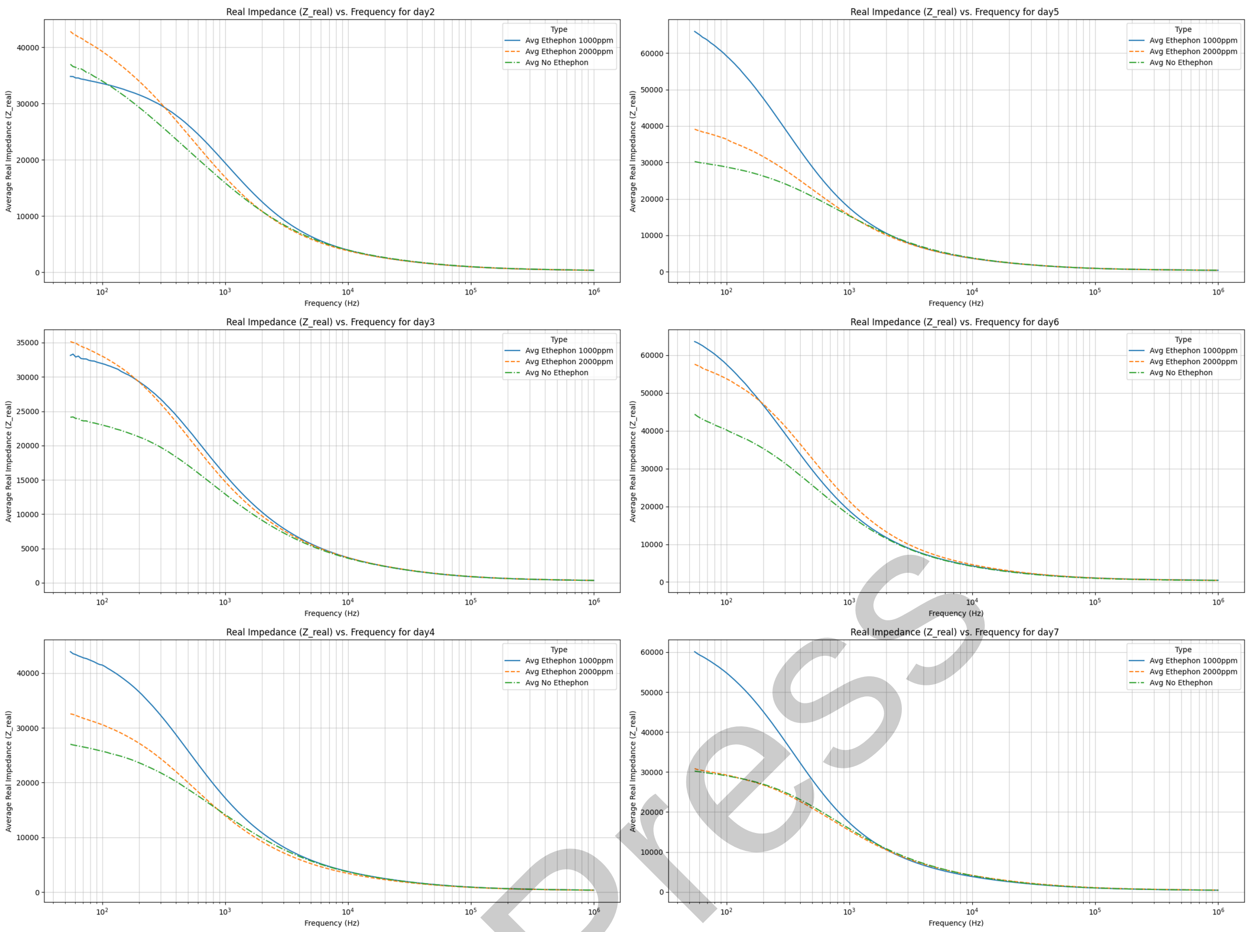

Fig. 16. Real Z over 6 days

structure, leading to the loss of the dielectric barrier. The resulting increase in membrane permeability facilitates the uncontrolled leakage of intracellular ions into the extracellular fluid, thereby reducing the overall insulation capacity of the tissue and increasing the mobility of free ions.

4.2. Validation of the Non-Invasive Framework

A critical achievement of this study is the demonstration of the superiority of the non-invasive measurement technique over traditional needle electrode methods. While invasive electrodes are prone to artifacts caused by localized tissue damage and wound responses, the use of flexible surface electrodes ensures that the acquired impedance spectrum reflects the natural physiological state of the specimen. The stability of the obtained data confirms that maintaining tissue integrity is essential for capturing an accurate "biological fingerprint" of the fruit.

Moreover, even though we've selected the most uniform samples for the experiment, there are still some undeniable differences in size and shape among the test subjects. Therefore, a fixed electrodes' position on the fruit surface may work for this small-scale experiment ($n = 12$), but can have negative impacts on larger sample size, affecting the validity of the overall outcome. Implementation should consider further factors including a larger number of specimens and the fluctuations in size, shape and weight of those, as well as their correlation to the electrode's placement and overall outcomes, ensuring a universal comparative view.

Besides that, the utilization of Ag/AgCl electrodes with a wet layer was specifically chosen to mitigate the effects of surface irregularities and minor humidity variations. Nevertheless, the observed 20% fluctuation in environment humidity represents a variable that could impact the peel conductivity, and tighter environmental controls will be implemented in the upcoming iterations.

4.3. Equivalent Circuit and Kinetic Characterization

The high degree of concordance between the experimental data and the modified Hayden equivalent circuit model validates the essential role of non-ideal capacitive elements in accurately characterizing fruit ripening kinetics. The inclusion of a Constant Phase Element (CPE) was necessary to account for the non-ideal capacitive behavior of the cell membranes and the heterogeneous structure of the fruit. Furthermore, the incorporation of Warburg impedance (W) provided critical insights into the diffusion of ions and metabolites within the parenchyma during the starch-to-sugar conversion.

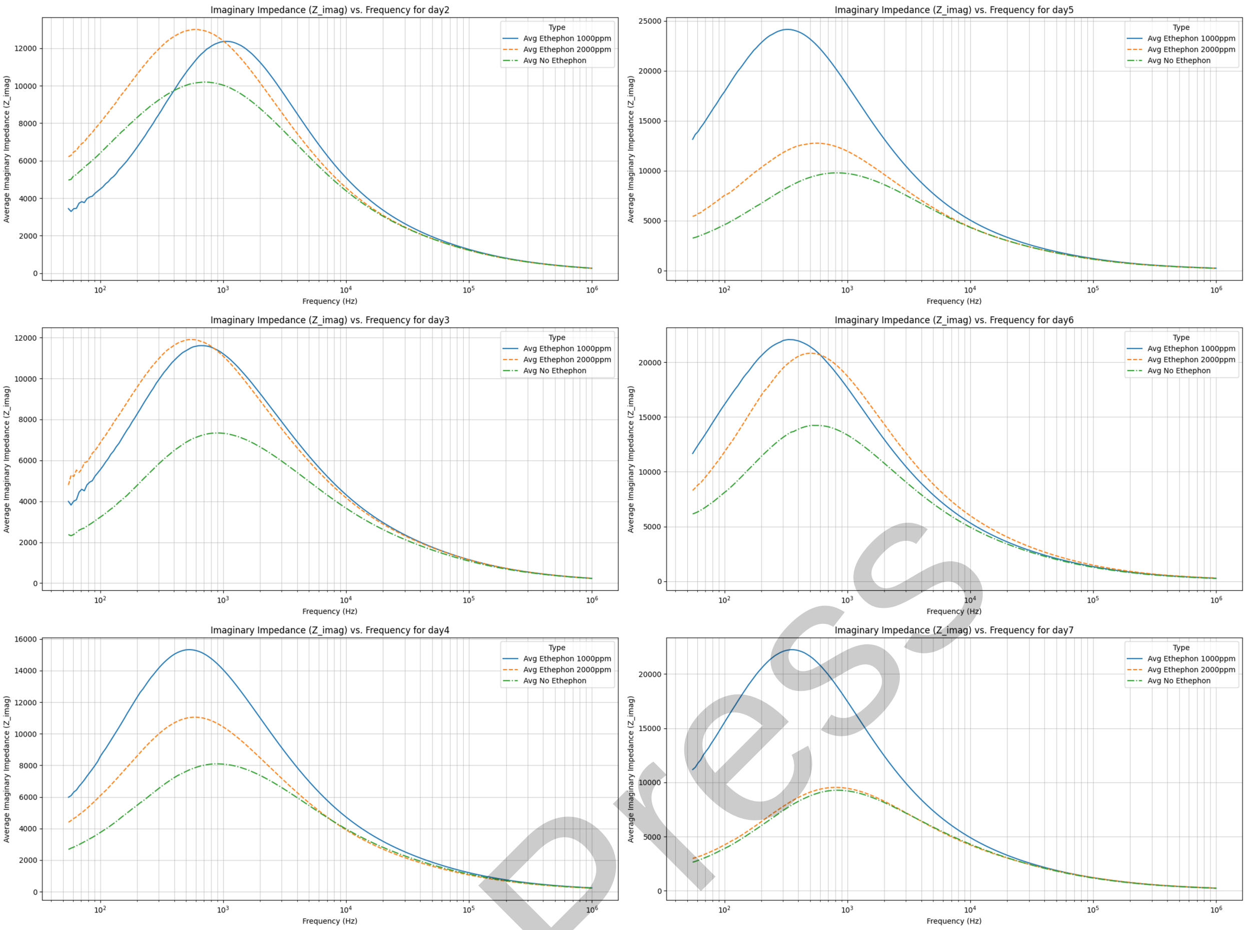

Fig. 17. Imaginary impedance (Z_{imag}) over 6 Days

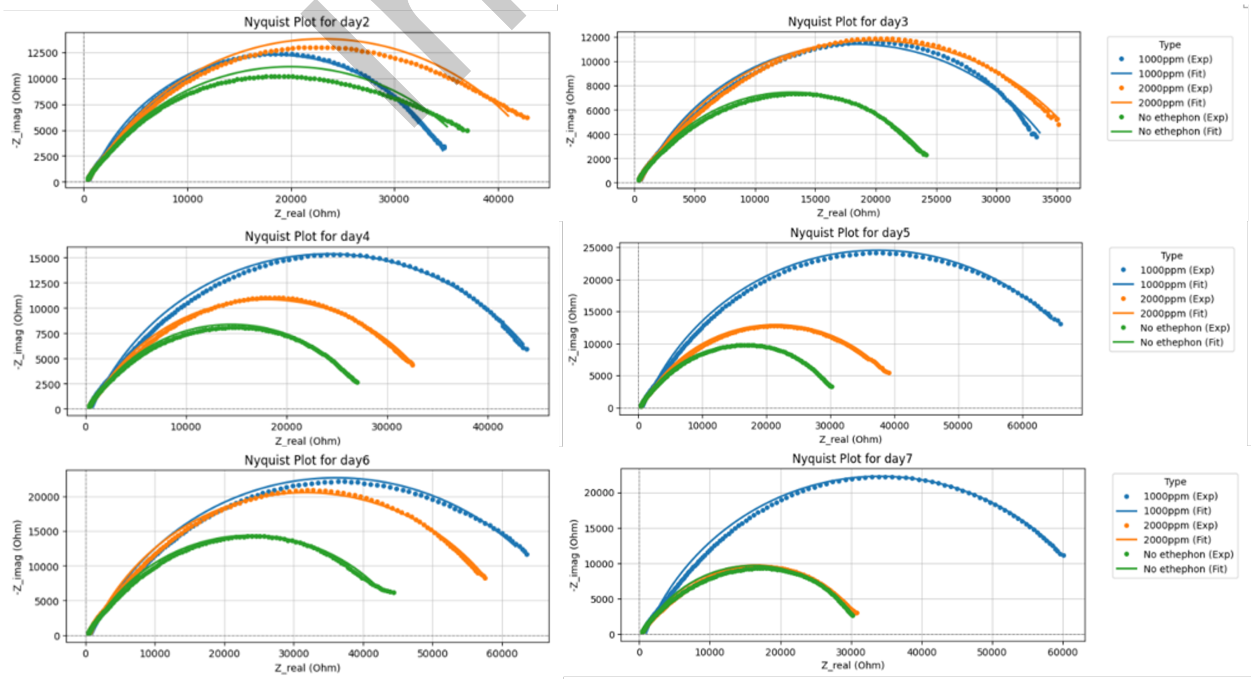

Fig. 18. Nyquist plot combine before and after fitting with equivalent circuit

These findings establish a reliable foundation for non-destructive agricultural quality monitoring applications. The ability to distinguish between natural ripening and chemical over-dosage through objective dielectric markers offers a rapid and cost-effective solution for quality control and ripening provenance detection in the modern agrifood supply chain.

5. Conclusion

This study establishes non-invasive Electrical Impedance Spectroscopy (EIS) as a robust analytical framework for monitoring banana ripening and identifying chemically induced acceleration. Through wide-band frequency analysis and surface electrode implementation, the approach successfully captured distinct dielectric patterns associated with varying Ethephon concentrations. The results demonstrate that moderate Ethephon application produces a consistent and progressive electrical response, whereas excessive concentration generates a markedly altered impedance trajectory, enabling clear differentiation between controlled ripening and overexposure.

These impedance-based signatures provide objective and quantifiable markers for assessing ripening progression without damaging the fruit. The strong agreement between experimental measurements and the proposed equivalent circuit model further confirms the suitability of dielectric modeling for characterizing internal tissue dynamics in a non-destructive manner. Collectively, the findings support the feasibility of EIS as a rapid, cost-effective tool for fruit quality assessment and ripening provenance verification within modern agri-food monitoring systems.

Future work will focus on improvising the limitations of the existing proof-of-concept by expanding the scale of the specimens, normalizing the framework for data acquisition, tightening environmental factors control, and transitioning from laboratory-grade instruments to a miniature, portable EIS device, enabling the research and application of a precise, real-time, field-based, end-to-end framework for food safety surveillance.

References

[1] M. Grossi and B. Riccò, Electrical impedance spectroscopy (EIS) for biological analysis and food characterization: a review, Journal of Sensors and Sensor Systems, vol. 6, no. 2, pp. 303–319, Aug. 2017. https://doi.org/10.5194/jsss-6-303-2017.

[2] Á. Kertész, Z. Hlaváčová, E. Vozáry, and L. Staroňová, Relationship between moisture content and electrical impedance of carrot slices during drying, International Agrophysics, vol. 29, no. 1, pp. 61–66, 2015. https://doi.org/10.1515/intag-2015-0013.

[3] X. Zhao, H. Zhuang, S. C. Yoon, Y. Dong, W. Wang, and W. Zhao, Electrical impedance spectroscopy for quality assessment of meat and fish: A review on basic principles, measurement methods, and recent advances, Journal of Food Quality, vol. 2017, p. 6370739, Jul. 2017. https://doi.org/10.1155/2017/6370739

[4] J.-L. Damez, S. Clerjon, S. Abouelkaram, and J. Lepetit, Beef meat electrical impedance spectroscopy and freshness assessment, Journal of Food Engineering, vol. 79, no. 1, pp. 120–150, 2007.

[5] K. N. Phan, V. A. Tran, D. T. Trung, and T. A. Duong, A novel method to determine the bio-impedance, International Journal of Science and Research), vol. 6, no. 10, pp. 649–654, Oct. 2017. https://doi.org/10.21275/ART20177209

[6] K. N. Phan, V. T. Anh, T. D. Thanh, and T. P. Xuan, Upgrade and Complete the Electrical Impedance Measuring System Applying for Meat Quality Analysis and Evaluation, vol. 243, May. 2021. https://doi.org/10.1007/978-981-16-2094-2_36.

[7] S. Grimnes and O. G. Martinsen, Bioimpedance and Bioelectricity Basics, 3rd ed., Academic Press, 2014.

[8] P. Ibba, A. Falco, B. D. Abera, G. Cantarella, L. Petti, and P. Lugli, Bio-impedance and circuit parameters: An analysis for tracking fruit ripening, Postharvest Biology and Technology, vol. 159, p. 111000, Jan. 2020. https://doi.org/10.1016/j.postharvbio.2019.110978

[9] S. G. Kulkarni, V. B. Kudachikar, and M. N. Keshava Prakash, Studies on physico-chemical changes during artificial ripening of banana (Musa sp.) variety 'Robusta', Journal of Food Science and Technology, vol. 48, no. 6, pp. 730–734, Oct. 2011. https://doi.org/10.1007/s13197-010-0133-y

[10] General Office of Statistics (GSO) & MARD, Vietnam Agricultural Statistical Yearbook 2023, Hanoi, Vietnam 2023.

[11] M. A. Hakim, A. K. Huq, M. D. Alam, A. Khatib, B. K. Saha, K. M. F. Haque, and M. Z. I. Sarker, Role of health hazardous ethephon in nutritive values of selected pineapple, banana, and tomato, Journal of Food, Agriculture & Environment, vol. 10, no. 2, pp. 247–251, Apr. 2012.

[12] A. Chowdhury, T. K. Bera, D. Ghoshal, and B. Chakraborty, Electrical impedance variations in banana ripening: an analytical study with electrical impedance spectroscopy, Journal of Food Process Engineering, vol. 40, no. 2, p. e12387, Jun. 2017. https://doi.org/10.1111/jfpe.12387

[13] M. Vemula, A. S. Sadiq, V. Mehtab, S. Chilakala, S. Chenna, V. Upadhyayula, and M. Tallapally, GC-MS based targeted metabolomics approach for studying the variations of phenolic metabolites in artificially ripened banana fruits, LWT - Food Science and Technology, vol. 130, p. 109622, Aug. 2020. https://doi.org/10.1016/j.lwt.2020.109622

[14] B. Li, J. Lecourt, and G. Bishop, Advances in Non-Destructive Early Assessment of Fruit Ripeness towards Defining Optimal Time of Harvest and Yield Prediction—A Review, Plants, vol. 7, no. 1, p. 3, Jan. 2018. https://doi.org/10.3390/plants7010003

[15] A. D. Bauchot, F. R. Harker, and W. M. Arnold, The use of electrical impedance spectroscopy to assess the physiological condition of kiwifruit, Postharvest Biology and Technology, vol. 18, no. 1, pp. 9–18, Jan. 2000. https://doi.org/10.1016/S0925-5214(99)00056-3